

Zinc(II) and Cadmium(II) *N,N*-Bis(2-*N*-Tosylaminobenzylidene)diaminodipropylimimates: Syntheses, Structures, and Photoluminescence Properties

T. P. Lysakova^a, A. S. Burlov^{b,*}, V. G. Vlasenko^b, Yu. V. Koshchienko^a, G. G. Aleksandrov^{c,†}, S. I. Levchenkov^d, Ya. V. Zubavichus^e, A. S. Cheprasov^d, D. A. Garnovskii^d, and A. V. Metelitsa^a

^aResearch Institute of Physical and Organic Chemistry, Southern Federal University, Rostov-on-Don, Russia

^bResearch Institute of Physics, Southern Federal University, Rostov-on-Don, Russia

^cKurnakov Institute of General and Inorganic Chemistry, Russian Academy of Sciences, Moscow, 119991 Russia

^dSouthern Scientific Center, Russian Academy of Sciences, Rostov-on-Don, Russia

^eNational Research Center “Kurchatov Institute”, Moscow, 123182 Russia

*e-mail: anatoly.burlov@yandex.ru

Received January 11, 2016

Abstract—Chemical and electrochemical syntheses of the zinc(II) and cadmium(II) complexes with the tetradentate Schiff base (H_2L), the condensation product of 2-*N*-tosylaminobenzaldehyde with diaminodipropylamine, are carried out. The structures, compositions, and properties of the synthesized metal complexes are studied by elemental analyses, IR spectroscopy, 1H NMR, UV spectroscopy, X-ray absorption spectroscopy, and quantum-chemical calculations. The structure of the cadmium(II) complex is determined by X-ray diffraction analysis (CIF file CCDC no. 1446393). The cadmium(II) and zinc(II) complexes exhibit luminescence in a CH_2Cl_2 solution in the blue spectral range ($\lambda_{PL} = 425–428$ nm) with the photoluminescence quantum yields $\varphi = 0.20$ and 0.75, respectively.

Key words: tetradeятate Schiff bases, zinc(II) and cadmium(II) complexes, X-ray diffraction analysis, photoluminescence

DOI: 10.1134/S1070328416110075

INTRODUCTION

Interest in zinc complexes with organic ligands is due to their biological activity and other important useful properties. The complexes possess antibacterial and antimicrobial properties [1, 2], exhibit high anti-tumor activity [3–12], and have hypoglycemic [13, 14] and radioprotective [15] properties.

The zinc (II) and cadmium(II) complexes with tetradeятate azomethine ligands based on 2-hydroxybenzaldehyde are also efficient metal-containing luminophores [16–28]. They demonstrate good photoluminescence (PL) and electroluminescence (EL) properties, are synthetically available, can easily be structurally modified for the optimization of their PL and EL characteristics, and form thin uniform films by thermal vacuum deposition. The devices based on organic light-emitting diodes (OLED) containing the zinc complexes of tetradeятate Schiff bases as emission layers in the short-wavelength range ($\lambda_{PL} = 440–510$ nm), and their

brighness is higher than 1400 cd/m² at a voltage of 16 V [16]. $[N,N'$ -Bis(salicylidene)-3,6-dioxa-1,8-diaminoctanate]zinc(II) monohydrate with the ZnN_2O_2 coordination core emitting in the blue range was synthesized and structurally characterized [23, 24]. The OLED devices with the electroluminescent layer based on this complex are characterized by the luminosity higher than 750 cd/m² and a threshold switch voltage of 4.5 V.

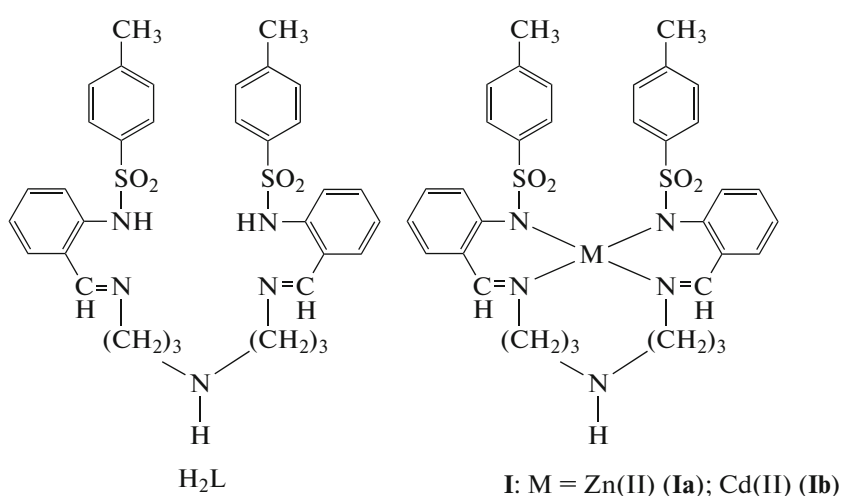
The zinc(II) and cadmium(II) complexes with the tetradeятate azomethine ligands, 2-*N,N*-bis(2-*N*-tosylaminobenzal)-3,6-dioxy-1,8-octadiamine and *N,N*-bis(2-*N*-tosylaminobenzal)-4,9-dioxo-1,12-dodecanediamine, having PL properties were synthesized and structurally characterized [29]. The complexes luminesce in a dimethylformamide solution in the blue spectral range ($\lambda_{PL} = 425–433$ nm) with the PL quantum yields $\varphi = 0.25–0.3$.

The search for new photo- and electroluminescent zinc and cadmium complexes with azomethine ligands remains to be an important and urgent task.

[†] Deceased.

This work is devoted to the chemical (CS) and electrochemical (ECS) syntheses of new zinc(II) and cadmium(II) complexes, **(Ia)** and **(Ib)**, with the tetradentate azomethine ligand, *N,N'*-bis(2-*N*-tosylaminobenzal)diaminodipropylamine (H_2L), having the PL properties. The replacement of the hydroxy group

in the aldehyde moiety by the 2-*N*-tosylamino group in the azomethine molecule H_2L affords respective metallochelates with the MN_4 coordination set, which should undoubtedly affect their structures and PL properties [26–28].



EXPERIMENTAL

2-*N*-Tosylaminobenzaldehyde was prepared by a described procedure [30].

Azomethine H_2L used for the syntheses of complexes **Ia** and **Ib** was synthesized by the condensation of 2-*N*-tosylaminobenzaldehyde and diaminodipropylamine.

Synthesis of H_2L . Diaminodipropylamine (1.32 g, 0.005 mol) was added to a solution of 2-*N*-tosylaminobenzaldehyde (2.75 g, 0.01 mol) in ethanol (50 mL). The mixture was stirred at room temperature for 2 h. A yellow precipitate formed upon cooling was filtered off and recrystallized from acetonitrile. The yield of pale yellow crystals of H_2L was 79%, mp = 109–110°C.

For $C_{34}H_{39}N_5O_4S_2$,

anal. calcd., %: C, 63.23; H, 6.09; N, 10.84.
Found, %: C, 63.31; H, 6.01; N, 10.72.

1H NMR (300 MHz, $CDCl_3$), δ , ppm: 1.85 br.s (4H, $2CH_2$), 2.34 s (6H, $2CH_3$), 2.56 br.s (4H, $2CH_2$), 3.47 br.s (4H, $2CH_2$), 6.99 t (2H, $J = 7.5$ Hz, C_{Ar-H}), 7.18–7.23 m (10H, C_{Ar-H}), 7.59 d (2H, $J = 8.1$ Hz, C_{Ar-H}), 7.69 s (2H, C_{Ar-H}), 7.72 s (2H, $CH=N$), 8.21 br.s (1H, NH).

IR, ν , cm^{-1} : 3334 w (NH), 1630 s ($CH=N$), 1286 m (as, SO_2), 1156 vs (s, SO_2). Absorption spec-

trum (CH_2Cl_2), λ , nm (ϵ , $L\ mol^{-1}\ cm^{-1}$): 258 sh, 312 (5200).

Synthesis of complexes **Ia and **Ib** by the chemical method (CS).** A solution of zinc acetate dihydrate (0.219 g, 0.001 mol) in methanol (5 mL) or cadmium acetate dihydrate (0.266 g, 0.001 mol) in methanol (5 mL) was added to a solution of H_2L (0.64 g, 0.01 mol) in methanol (20 mL). The mixture was stirred at room temperature for 3 h. A precipitate formed was filtered off, recrystallized from a methanol–dichloromethane (2 : 1) mixture, and dried in a vacuum desiccator at 150°C.

Synthesis of complexes **Ia and **Ib** by the electrochemical method (ECS).** An electrochemical cell with the platinum cathode and zinc (or cadmium) anode was filled with a solution of H_2L (0.64 g, 0.001 mol) in acetonitrile (20 mL), and $[Et_4N]ClO_4$ (0.01 g) was added as a conducting additive. The electrosynthesis was carried out at a current strength of 40 mA and a voltage of 20 V for 1 h at room temperature. A precipitate of the complex formed was filtered off, recrystallized from a methanol–dichloromethane (2 : 1) mixture, and dried in a vacuum desiccator at 150°C.

Cathode (Pt): $LH_2 + 2e \rightarrow L^{2-} + H_2$.

Anode: (Zn^0 or Cd^0) $M - 2e \rightarrow M^{2+}$ ($M = Zn, Cd$).

Solution: $L^{2-} + M^{2+} \rightarrow ML$.

The yields of white crystals of compound **Ia** were 81% (CS) and 91% (ECS), mp = 291–292°C.

For $C_{34}H_{37}N_5O_4S_2Zn$

anal. calcd., %: C, 57.58; H, 5.26; N, 9.87; Zn, 9.22.
Found, %: (CS) C, 57.62; H, 5.19; N, 9.80; Zn, 9.32.
(ECS) C, 57.60; H, 5.10; N, 9.90; Zn, 9.30.

1H NMR (300 MHz, $CDCl_3$), δ , ppm: 1.93–1.95 m (4H, 2CH₂), 2.24 s (6H, 2CH₃), 3.20–3.31 m (4H, 2CH₂), 3.53–3.55 m (4H, 2CH₂), 6.48 s (2H, C_{Ar-H}), 6.61–6.63 m (2H, C_{Ar-H}), 6.68–6.71 m (2H, C_{Ar-H}), 6.99 d (4H, J = 8.3 Hz, C_{Ar-H}), 7.08–7.10 s (2H, C_{Ar-H}), 7.37 d (4H, J = 8.1 Hz, C_{Ar-H}), 8.12 s (2H, CH=N).

IR, ν , cm^{-1} : 3286 w (NH), 1639 s (CH=N), 1246 s (as, SO₂), 1130 vs (s, SO₂). Absorption spectrum (CH_2Cl_2), λ , nm (ϵ , L mol⁻¹ cm⁻¹): 270 sh, 352 (3700).

The yields of white crystals of complex **Ib** were 58% (CS) and 72% (ECS), mp = 284–285°C.

For $C_{34}H_{37}N_5O_4S_2Cd$

anal. calcd., %: C, 54.00; H, 4.93; N, 9.26; Cd, 14.86.
Found, %: (CS) C, 54.08; H, 4.87; N, 9.28; Cd, 14.91.
(ECS) C, 54.05; H, 4.75; N, 9.20; Cd, 14.95.

1H NMR (300 MHz, $CDCl_3$), δ , ppm: 1.81–1.87 m (3H, CH₂), 2.26 s (3H, CH₃), 2.29 s (3H, CH₃), 2.30–2.38 m (2H, CH₂), 2.53–2.55 m (1H, CH₂), 2.97–3.08 m (3H, CH₂), 3.32–3.34 m (1H, CH₂), 3.55–3.57 m (1H, CH₂), 3.62–3.64 m (1H, CH₂), 3.98 s + d (1H, $^3J_{Cd-H}$ = 18.3 Hz, CH=N), 4.50–4.52 m (1H, NH), 6.68–6.73 m (2H, C_{Ar-H}), 6.95–6.97 m (1H, C_{Ar-H}), 7.07–7.14 m (7H, C_{Ar-H}), 7.23–7.24 m (1H, C_{Ar-H}), 7.43 d (1H, J = 8.4 Hz, C_{Ar-H}), 8.07 t (4H, J = 7.8 Hz, C_{Ar-H}), 8.18 s + d (1H, $^3J_{Cd-H}$ = 15.4 Hz, CH=N).

IR, ν , cm^{-1} : 3347 w (NH), 1637 s (CH=N), 1282 s (as, SO₂), 1127 vs (s, SO₂). Absorption spectrum (CH_2Cl_2), λ , nm (ϵ , L mol⁻¹ cm⁻¹): 275 sh, 350 (6500).

C, H, N elemental analyses were carried out on a Carlo Erba Instruments TCM 480 instrument. The IR spectra of the samples were recorded on a Varian 3100-FTIR Excalibur instrument in a range of 4000–400 cm^{-1} using the attenuated total internal reflectance (ATR) method. 1H NMR spectra were detected on a VarianUnity 300 spectrometer with a working frequency of 300 MHz in the mode of internal stabilization of the 2H polar resonance line in $DMSO-d_6$ at 20°C. The absorption spectra of compounds **Ia** and **Ib** were recorded on Varian Cary 100 and Varian Cary 50 spectrophotometers in dichloromethane solutions.

The X-ray absorption Zn *K* edge of complex **Ia** in the solid state was detected in the transmission mode on an EXAFS spectrometer of the Structural Materials Science station at the Kurchatov Center of Synchrotron Radiation and Nanotechnologies (Moscow) [31]. The energy of the electron beam used as an X-ray synchrotron radiation source was 2.5 GeV at a current of 80–100 mA. A double crystal Si(111) monochromator was used for X-ray radiation monochromatization. The obtained absorption spectrum was processed using standard procedures of background subtraction, normalization to the value of the *K*-edge jump, and the isolation of atomic absorption μ_0 , after which the Fourier transform of the obtained extended X-ray absorption fine structure (EXAFS) χ spectra was performed in the range of wave vectors of photoelectrons k from 3.0 to 13.0 \AA^{-1} with the weight function k^3 . The obtained module Fourier transformant (MFT) was the pseudoradial distribution of atoms of the nearest coordination spheres around the absorbing zinc atom with the values of radii of the coordination spheres obtained with the accuracy to phase corrections. The threshold ionization energy E_0 was chosen by the value of the maximum of the first derivative of the *K* edge and further was varied by fitting. The exact values for parameters of the nearest environment of the zinc ions in the compounds were determined by the nonlinear fitting of the parameters of the corresponding coordination spheres comparing the calculated EXAFS signal and the signal isolated from the full EXAFS spectrum by the Fourier filtration method. The nonlinear fitting was performed using the IFFEFIT-1.2.11 program package [32]. The phases and scattering amplitudes of the photoelectron wave necessary for the construction of the model spectrum were calculated using the FEFF7 program [33] and atomic coordinates of compounds with a similar atomic structure. The goodness-of-fit Q , which was minimized when determining the parameters of the nearest environment structure, was calculated by the formula

$$Q (\%) = \frac{\sum [k\chi_{\text{exp}}(k) - k\chi_{\text{th}}(k)]^2}{\sum [k\chi_{\text{exp}}(k)]^2} \times 100.$$

The quantum-chemical calculations of the optimized geometry of molecules of zinc and cadmium complexes **Ia** and **Ib** in the ground state were performed using the GAUSSIAN-03 program [34] in the density functional theory (DFT) approximation. The B3LYP hybrid three-parameter functional [35, 36] and the 6-31G(d) standard split valence polarization basis set [37] were chosen for the calculations (the LanL2DZ basis set was chosen for the Cd atom in complex **Ib** [38]). This calculation scheme was multiply used for the optimization of molecular structures of both organic compounds and metal complexes.

X-ray diffraction analysis for complex **Ib** was carried out on an Agilent Technologies Xcalibur E diffractom-

Table 1. Crystallographic data and experimental and refinement characteristics for compound **Ib**

Parameter	Value
<i>FW</i>	756.21
Crystal size, mm	0.32 × 0.09 × 0.08
Temperature, K	120(2)
Crystal system	Monoclinic
Space group	<i>P2₁/c</i>
<i>a</i> , Å	9.3306(5)
<i>b</i> , Å	31.4688(18)
<i>c</i> , Å	11.3838(7)
β, deg	95.5863(9)
<i>V</i> , Å ³	3326.7(3)
<i>Z</i>	4
ρ _{calcd} , g/cm ³	1.510
μ, mm ⁻¹	0.828
<i>F</i> (000)	1552
θ Range, deg	2.22–29.16
Number of measured reflections	27493
Number of independent reflections	8907
Number of reflections with <i>I</i> > 2σ(<i>I</i>)	7364
Ranges of reflection indices	–10 ≤ <i>h</i> ≤ 12, –43 ≤ <i>k</i> ≤ 42, –15 ≤ <i>l</i> ≤ 14
Number of refined parameters	415
<i>R</i> ₁ (<i>I</i> > 2σ(<i>I</i>))	0.0387
<i>wR</i> ₂ (all reflections)	0.1258
GOOF (all reflections)	1.001
Δρ _{max} /Δρ _{min} , eÅ ⁻³	1.25/–0.63

eter equipped with a CCD detector and a monochromatic radiation source (MoK_α radiation, $\lambda = 0.71073$ Å) using the CrysAlisPro standard procedure [39]. The structure was solved by a direct method and refined in the full-matrix anisotropic approximation for all non-hydrogen atoms. The hydrogen atoms in complex **Ib** were localized from the difference electron density syntheses and refined in the isotropic approximation. The main crystallographic data for complex **Ib** and refinement parameters are presented in Table 1. Selected interatomic distances and bond angles in the coordination polyhedra of the cadmium atoms in a molecule of complex **Ib** are given in Table 2.

All calculations were performed using the SHELXS-97 program package [40]. The X-ray diffraction data for compound **Ib** were deposited with the Cambridge Crystallographic Data Centre (CIF file CCDC no. 1446393; deposit@ccdc.cam.ac.uk or http://www.ccdc.cam.ac.uk/data_request/cif).

RESULTS AND DISCUSSION

Tetradeятate azomethine ligand H₂L was synthesized by the condensation of methanolic solutions of 2-*N*-tosylaminobenzaldehyde and diaminodipropylamine in a molar ratio of 2 : 1. Metal complexes **Ia** and **Ib** were obtained using two methods: CS with metal acetates and ECS by the anodic dissolution of zerovalent metals in an acetonitrile solution of azomethine H₂L.

The IR spectrum of H₂L exhibits a weakly intense absorption band at 3334 cm^{–1} caused by stretching vibrations of the NH groups of the amine moiety and intense absorption bands at 1630 ν (CH=N), 1286 ν_{as} (SO₂), and 1156 cm^{–1} ν_s (SO₂). The absorption bands of the tosylamine moieties bound by a strong intramolecular hydrogen bond are not observed in the IR spectra.

The ¹H NMR spectrum of H₂L in a CDCl₃ solution displays signals at 7.72 ppm from the protons of the CH=N groups and a broadened signal of the NH proton of the amine fragment at 8.21 ppm. The signals of the NH protons of the aldehyde fragments are not observed in the ¹H NMR spectra.

According to the elemental analyses data, complexes **Ia** and **Ib** have the ML composition regardless of the synthesis method. However, the yield of the complexes synthesized using the ECS is higher by approximately 10% compared to the CS.

The weak stretching vibration bands at 3342 (**Ia**) and 3286 cm^{–1} (**Ib**) corresponding to ν (NH) of the amine moiety of the ligand are retained in the IR spectra of the complexes. The ν (CH=N) absorption band at 1630 cm^{–1} of the ligand increases insignificantly from 1639 cm^{–1} for **Ia** and 1637 cm^{–1} for **Ib** upon the formation of complexes **Ia** and **Ib**. Significant changes upon complex formation are observed for the stretching vibration bands of HL₂ at 1286 cm^{–1} ν_{as} (SO₂) and 1156 cm^{–1} ν_s (SO₂), which decrease to 1246 (**Ia**), 1282 cm^{–1} (**Ib**) ν_{as} (SO₂) and 1130 (**Ia**), 1127 cm^{–1} (**Ib**) ν_s (SO₂), respectively.

In the ¹H NMR spectra of complexes **Ia** and **Ib**, signals of the protons of the secondary NH groups of the amine moiety of the ligand are observed at 8.12 (**Ia**) and 4.50–4.52 ppm (**Ib**). The signals of protons of the CH=N groups in complexes **Ia** and **Ib** undergo downfield shifts and are observed at 8.12 (**Ia**) and 8.18 ppm (**Ib**).

The atomic structure of complex **Ib** was determined by X-ray diffraction analysis. The local atomic structure of complex **Ia** was studied by X-ray absorption spectroscopy from analyses of X-ray absorption near edge structure (XANES) and EXAFS.

The configuration of the CdL molecule in the structure of complex **Ib** is presented in Fig. 1. The doubly deprotonated organic ligand is coordinated to

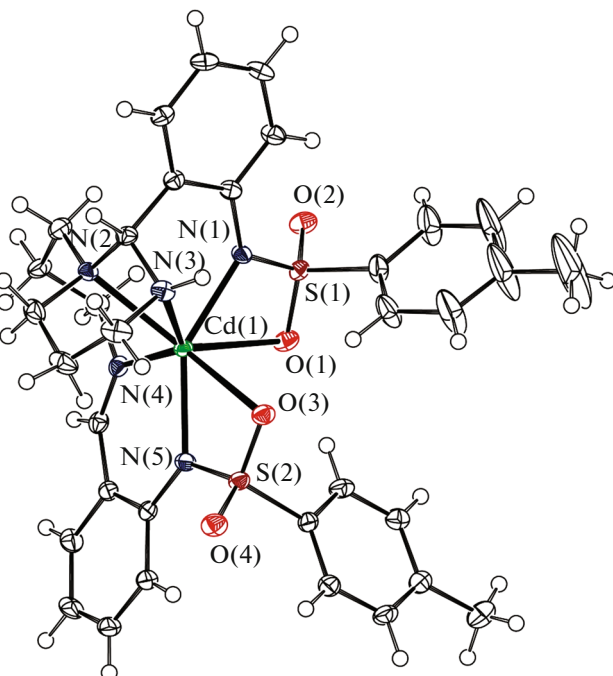
Table 2. Selected interatomic distances and bond angles in the coordination polyhedra of the cadmium atoms in a molecule of complex **Ib** according to the X-ray diffraction data

Bond	<i>d</i> , Å	Bond	<i>d</i> , Å
Cd(1)–N(1)	2.219(2)	Cd(1)–N(5)	2.245(2)
Cd(1)–N(2)	2.462(2)	Cd(1)–O(1)	2.690(2)
Cd(1)–N(3)	2.486(2)	Cd(1)–O(3)	2.580(2)
Cd(1)–N(4)	2.284(2)		
Angle	ω , deg	Angle	ω , deg
N(1)Cd(1)N(5)	146.11(9)	N(5)Cd(1)O(3)	58.91(7)
N(1)Cd(1)N(4)	107.12(8)	N(4)Cd(1)O(3)	139.23(8)
N(5)Cd(1)N(4)	81.48(8)	N(2)Cd(1)O(3)	132.28(7)
N(1)Cd(1)N(2)	84.69(8)	N(3)Cd(1)O(3)	78.56(7)
N(5)Cd(1)N(2)	129.17(8)	N(4)Cd(1)O(1)	84.31(8)
N(4)Cd(1)N(2)	79.30(8)	N(1)Cd(1)O(1)	57.17(8)
N(1)Cd(1)N(3)	80.69(8)	N(5)Cd(1)O(1)	92.34(8)
N(5)Cd(1)N(3)	117.53(8)	N(3)Cd(1)O(1)	131.94(7)
N(4)Cd(1)N(3)	133.72(8)	N(2)Cd(1)O(1)	131.42(7)
N(2)Cd(1)N(3)	55.60(7)	O(3)Cd(1)O(1)	87.77(6)
N(1)Cd(1)O(3)	101.70(7)		

the Cd²⁺ ion by five nitrogen atoms: azomethine N(2) and N(4) atoms, amine N(1) and N(5) atoms, and the N(2) atom of the diiminodipropylamine fragment (Table 2). Four six-membered metallacycles undergo ring closure upon coordination. The coordination polyhedron of the Cd atom can be described as a strongly distorted square pyramid the equatorial positions in which are occupied by the N(1), N(2), N(3), and N(4) atoms, and the N(5) atom is located in the apical position. In addition, the coordination to the Cd atom of the O(1) and O(3) oxygen atoms of the tosyl groups (Cd–O 2.690(2) and 2.580(2) Å, respectively), takes place in the complex, which increases the coordination number of the Cd²⁺ ion to seven [41–43].

The four-membered metallacycles Cd(1)N(1)S(1)O(1) and Cd(1)N(5)S(2)O(3) are nearly planar. The six-membered chelate Cd(1)N(4)C(14)C(15)C(20)N(5) (**A**) is somewhat distorted because of the shift of the N(5) atom from the plane of other five atoms by 0.176 Å. In two other six-membered metallacycles, Cd(1)N(1)C(1)C(6)C(7)N(2) and Cd(1)N(1)C(1)C(6)C(7)N(3), the N(2) and N(3) atoms shift from the planes of other five atoms by 1.098 and 1.203 Å, respectively. These three metallacycles have a sofa conformation (cycle **A** is flattened). One more six-membered chelate, Cd(1)N(2)C(8)C(9)C(10)N(3), exists in a chair conformation, and the Cd(1) and C(9) atoms shift from the mean plane of other four atoms by +1.188 and –0.711 Å, respectively.

The data on the local atomic structure of the zinc ions in compound **Ia** were obtained from analyses of XANES and EXAFS absorption Zn *K* edge of **Ia** (it turned out impossible to grow single crystals of this complex suitable for X-ray diffraction analysis). The

**Fig. 1.** Structure of complex **Ib** in representation of atoms by atomic shift ellipsoids with 30% probability.

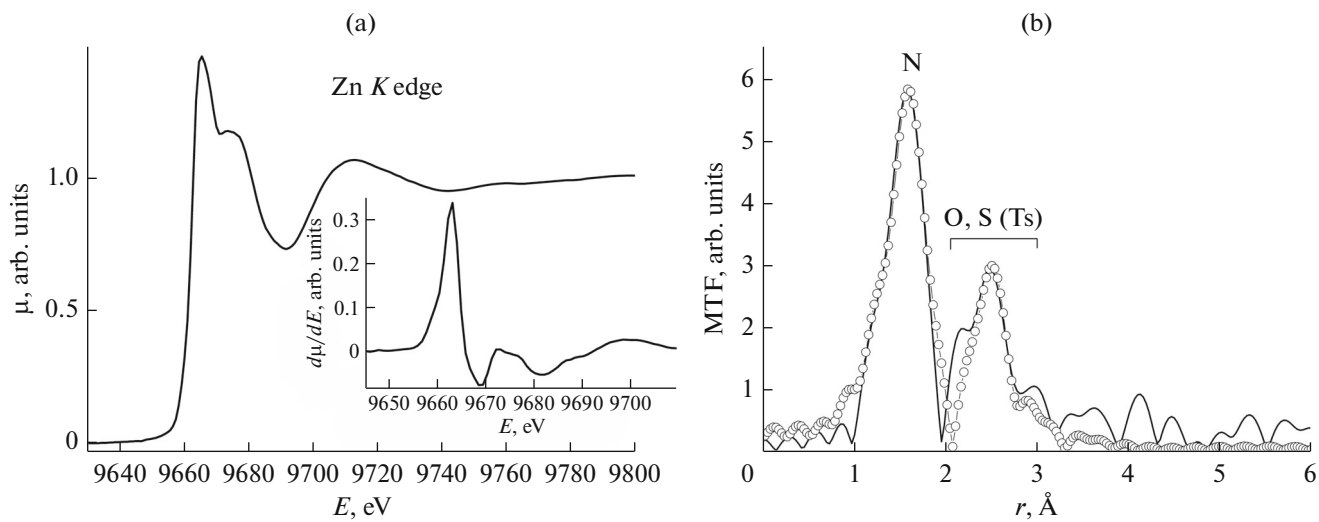


Fig. 2. (a) X-ray absorption Zn *K* edge and (b) MFT EXAFS for complex **Ia**: experiment is presented by solid line, and theory is shown by empty circles.

X-ray absorption Zn *K* edge and its first derivative for complex **Ia** are shown in Fig. 2a. The XANES shape and especially that of its first derivative consist of a broadened maximum and is typical of complexes with the tetrahedral environment of the absorbing atom. The XANES of Zn *K* edges of compound **Ia** almost has no pre-edge structure because of the completely filled 3*d* shell of the zinc atom.

The MFT of EXAFS for complex **Ia** has the major peak ($r = 1.60$ Å) unambiguously corresponding to scattering on the nearest coordination spheres consisting of the nitrogen atoms of the ligands and the peak at a long distance ($r = 2.52$ Å) corresponding to scattering on the subsequent coordination spheres (Fig. 2b).

The parameters of the local atomic environment of the zinc ion in complex **Ia** obtained for the best model of the coordination polyhedron with the minimum function $Q = 2.2\%$ (in the fitting range $\Delta r = 1$ –3 Å) correspond to the tetrahedral environment of four nitrogen atoms of ligands L^{2-} at an average distance of 2.05 Å. The second MFT peak corresponds to the coordination sphere consisting of the oxygen and sulfur atoms of two tosylamine fragments of the ligands at distances of 2.85–2.90 Å.

The DFT-optimized interatomic distances and angles between the bonds for molecules of compounds **Ia** and **Ib** are presented in Table 3. The distances and angles in a molecule of **Ib** obtained from the quantum-chemical calculations correspond well to the experimental values obtained by X-ray diffraction analysis. A comparative analysis of the selected geometric parameters demonstrates that the average deviation for distances does not exceed 0.02 Å (ignoring Cd(1)–N(2) for which the deviation is anomalously high (~0.17 Å)) and that for angles is not higher than 3°. For complex **Ia**, the calculated average dis-

tance of four nearest bonds Zn–N (2.0569 Å) is consistent with the radius of the first coordination sphere equal to 2.05 Å, which was obtained from the X-ray spectral data for this compound.

The absorption and PL spectra of complexes **Ia** and **Ib** are presented in Fig. 3. A long-wavelength absorption band at ~350 nm and a shoulder at the slope of the intense absorbance at 270–275 nm are observed in the absorption spectra of the complexes in dichloromethane. The long-wavelength bands undergo a significant (~40 nm) bathochromic shift compared to a similar band (312 nm) of azomethine H_2L .

To interpret the absorption spectra of complexes **Ia** and **Ib**, we performed the quantum-chemical calculations of the singlet excited electron states of these molecules using the time-dependent density functional theory (TD-DFT) method and taking into account solvation effects.

The theoretical absorption spectra compared with experimental ones are shown in Fig. 3. The calculated wavelengths λ , energies of vertical electron transitions E between the corresponding molecular orbitals (MO), contributions of individual electron transitions, and oscillator forces f for complexes **Ia** and **Ib** obtained from the TD-DFT/B3LYP/LANL2DZ calculations are given in Table 4. The calculated bands for complex **Ia** coincided with experiment with an accuracy to several nm, whereas the theoretical absorption band of complex **Ib** is shifted by ~15 nm relative to the experimental maxima. This shift is likely caused by the use of the split-valence basis set with the LanL2DZ effective potential of the core for the Cd atom.

The data of the TD-DFT calculations for complexes **Ia** and **Ib** (Table 4) showed that the long-wavelength absorption band was due to singlet-singlet electron transitions among which the HOMO \rightarrow LUMO

Table 3. Optimized parameters of the atomic structure for molecules of complexes **Ia** and **Ib**

Ia		Ib	
Bond	<i>d</i> , Å	Bond	<i>d</i> , Å
Zn(1)–N(1)	2.0082	Cd(1)–N(1)	2.2277
Zn(1)–N(2)	2.6484	Cd(1)–N(2)	2.6279
Zn(1)–N(3)	2.1463	Cd(1)–N(3)	2.4770
Zn(1)–N(4)	2.0545	Cd(1)–N(4)	2.3081
Zn(1)–N(5)	2.0185	Cd(1)–N(5)	2.2430
Zn(1)–O(1)	2.7222	Cd(1)–O(1)	2.6515
Zn(1)–O(3)	2.7439	Cd(1)–O(3)	2.6130
Angle	ω , deg	Angle	ω , deg
N(1)Zn(1)N(5)	141.55	N(1)Cd(1)N(5)	152.64
N(1)Zn(1)N(4)	105.70	N(1)Cd(1)N(4)	108.93
N(5)Zn(1)N(4)	92.30	N(5)Cd(1)N(4)	81.35
N(1)Zn(1)N(2)	89.02	N(1)Cd(1)N(2)	82.46
N(5)Zn(1)N(2)	128.62	N(5)Cd(1)N(2)	124.88
N(4)Zn(1)N(2)	76.66	N(4)Cd(1)N(2)	77.33
N(1)Zn(1)N(3)	90.23	N(1)Cd(1)N(3)	80.29
N(5)Zn(1)N(3)	103.86	N(5)Cd(1)N(3)	113.20
N(4)Zn(1)N(3)	130.16	N(4)Cd(1)N(3)	129.83
N(2)Zn(1)N(3)	56.30	N(2)Cd(1)N(3)	54.50
N(1)Zn(1)O(3)	91.80	N(1)Cd(1)O(3)	99.04
N(5)Zn(1)O(3)	60.08	N(5)Cd(1)O(3)	63.48
N(4)Zn(1)O(3)	149.86	N(4)Cd(1)O(3)	143.31
N(2)Zn(1)O(3)	128.99	N(2)Cd(1)O(3)	130.83
N(3)Zn(1)O(3)	72.69	N(3)Cd(1)O(3)	77.12
N(4)Zn(1)O(1)	83.50	N(4)Cd(1)O(1)	90.45
N(1)Zn(1)O(1)	60.14	N(1)Cd(1)O(1)	62.54
N(5)Zn(1)O(1)	89.44	N(5)Cd(1)O(1)	92.87
N(3)Zn(1)O(1)	142.08	N(3)Cd(1)O(1)	133.29
N(2)Zn(1)O(1)	137.01	N(2)Cd(1)O(1)	136.94
O(3)Zn(1)O(1)	84.36	O(3)Cd(1)O(1)	81.67

and HOMO-1 → LUMO intense transitions with the highest oscillator force *f* are determining. As already established multiply by the analysis of the absorption spectra of similar zinc and cadmium complexes, the nature of this band can be interpreted as an interligand charge transfer caused by the electron transitions from the π -bonding orbital (HOMO) to the π^* -antibonding orbital (LUMO) of the ligands. As can be seen from Fig. 4, the HOMO in complexes **Ia** and **Ib** has the maximum contribution of the π component of the MO of the azomethine fragment of the ligand, as well as the π^* -antibonding part of the LUMO, while the tosylamine fragments do not contribute to the HOMO and LUMO of the molecules. A set of electron transitions corresponds to the absorption band at 270–275 nm. Among these electron transitions, the determining are

HOMO-3 → LUMO, HOMO → LUMO+5, and HOMO-5 → LUMO for complex **Ia** and HOMO-1 → LUMO+1 and HOMO → LUMO+4 for complex **Ib**.

The photoexcitation of the complexes ($\lambda_{\text{exc}} = 320$ nm) induces an emission PL band ($\lambda_{\text{max}} = 425$ nm (**Ia**) and $\lambda_{\text{PL}} = 433$ nm (**Ib**)), unlike nonluminescent azomethine compound H_2L . The fluorescence excitation spectra coincide well with the corresponding absorption spectra, indicating that the fluorescence bands of complexes **Ia** and **Ib** were assigned correctly. The fluorescence of the complexes is characterized by a high efficiency with the quantum yields $\varphi = 0.75$ (**Ia**) and 0.2 (**Ib**).

Complexes **Ia** and **Ib** are thermally stable, their mp are higher than 280°C, and they can find use, accord-

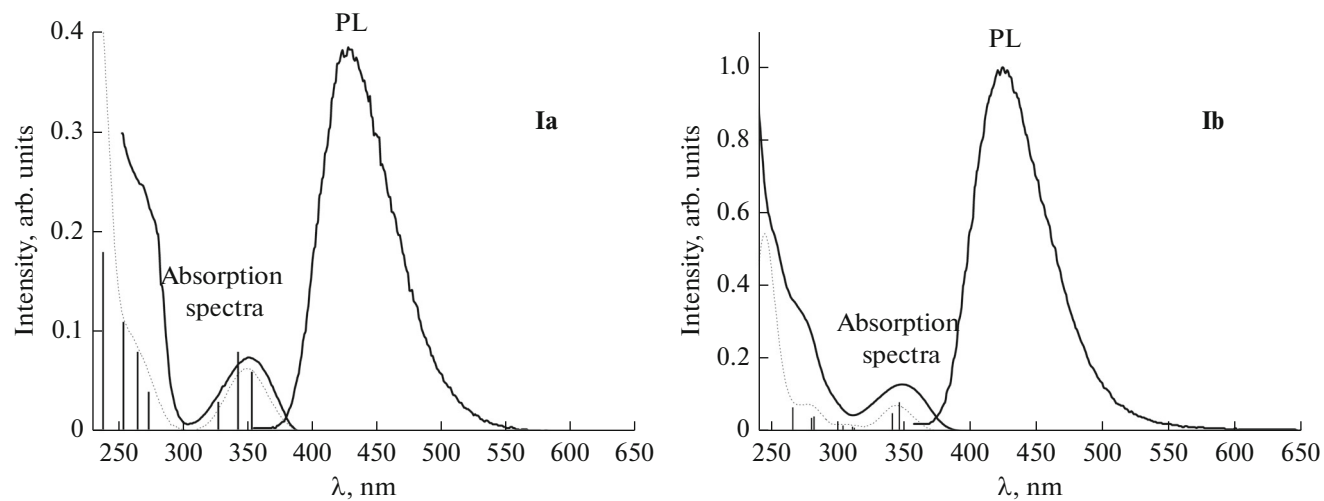


Fig. 3. Absorption and photoluminescence spectra of complexes **Ia** and **Ib** (theoretical absorption spectra are shown by dotted lines).

Table 4. Calculated wavelengths λ , energies of vertical electron transitions E between the corresponding MO, contributions of individual electron transitions, and oscillator forces f for complexes **Ia** and **Ib** obtained from the TD-DFT calculations

Ia				Ib			
λ , nm	E , eV	Electron transitions, (contributions**, %)	f	λ , nm	E , eV	Electron transitions, (contributions**, %)	f
353.01 (352)*	3.512	HOMO → LUMO (85%) HOMO-1 → LUMO (10%)	0.06	331.89 (350)*	3.74	HOMO → LUMO (52%) HOMO-1 → LUMO (40%)	0.08
342.35	3.622	HOMO-1 → LUMO (79%) HOMO → LUMO (13%)	0.08	326.66	3.80	HOMO-1 → LUMO (48%) HOMO → LUMO (47%)	0.05
327.09	3.791	HOMO-2 → LUMO (92%)	0.03	297.93	4.16	HOMO-2 → LUMO (87%)	0.01
273.20 (270)*	4.538	HOMO-3 → LUMO (76%)	0.04	289.40	4.28	HOMO-1 → LUMO+1 (70%) HOMO-1 → LUMO+2 (22%)	0.02
264.64	4.685	HOMO → LUMO+5 (74%)	0.08	267.57 (275)*	4.63	HOMO → LUMO+3 (30%) HOMO → LUMO+4 (55%)	0.04
253.63	4.889	HOMO-5 → LUMO (46%) HOMO-4 → LUMO (10%) HOMO-1 → LUMO+6 (14%)	0.11	251.54	4.93	HOMO-1 → LUMO+6 (33%) HOMO-4 → LUMO (27%) HOMO-6 → LUMO (10%)	0.07
237.86	5.213	HOMO-2 → LUMO+3 (16%) HOMO → LUMO+6 (34%) HOMO → LUMO+7 (23%)	0.18	239.32	5.18	HOMO → LUMO+6 (57%) HOMO → LUMO+7 (21%)	0.12

* Experimental values.

** Only contributions higher than 10%.

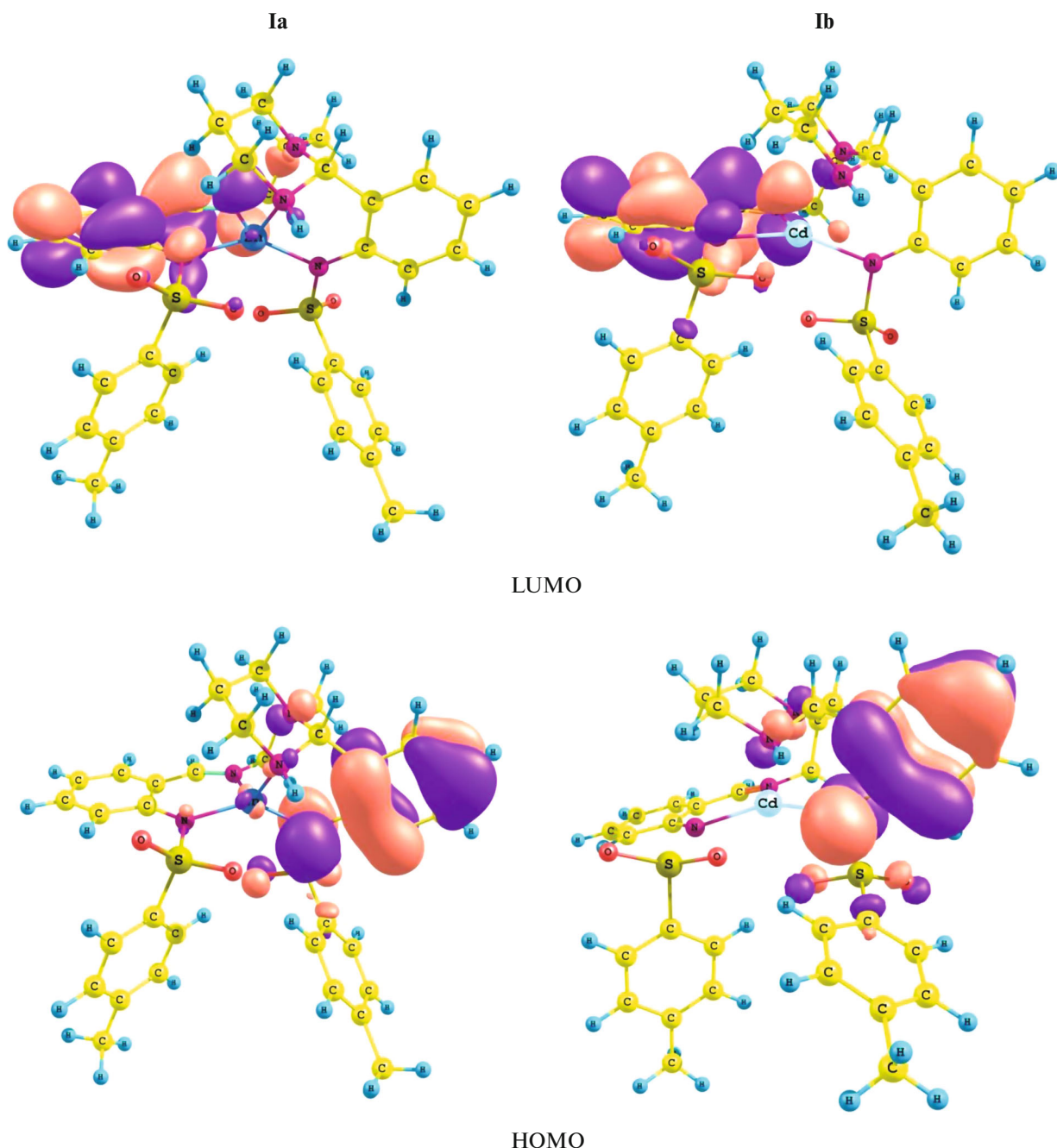


Fig. 4. Isosurfaces of the HOMO and LUMO for complexes Ia and Ib.

ing to their characteristics, as emission layers in the production of OLED devices.

ACKNOWLEDGMENTS

The IR and ^1H NMR experimental data were obtained using the equipment of the Shared Facility Center at the Southern Federal University (Rostov-on-Don, Russia). The Unique Research System “Kurchatov Synchrotron Radiation Source” financed by the Ministry of Education and Science of the Russian

Federation (project identifier RFME-FI61914X0002) was used.

This work was carried out in the framework of the design part of the state program in the sphere of scientific activities (project no. 4.742.2014/K).

REFERENCES

1. Chohan, Z.H., Arif, M., and Sarfraz, M., *Appl. Organomet. Chem.*, 2007, vol. 21, p. 294.

2. Kaczmarek, M.T., Jastrza, R., Holderna-Kedzia, E., and Radecka-Paryzek, W., *Inorg. Chim. Acta*, 2009, vol. 362, p. 3127.
3. Huang, Q., Pan, Z., Wang, P., et al., *Bioorg. Med. Chem. Lett.*, 2006, vol. 16, p. 3030.
4. Miyamoto, D., Endo, N., Oku, N., et al., *Biol. Pharm. Bull.*, 1998, vol. 21, p. 1258.
5. Belicchi, FerrariM., Bisceglie, F., Pelosi, G., et al., *J. Inorg. Biochem.*, 2001, vol. 87, p. 137.
6. Beraldo, H. and Gambino, D., *Mini-Rev. Med. Chem.*, 2004, vol. 4, p. 31.
7. Rodriguez-Arguelles, M.C., Belichi Ferrari, M., Bisceglie, F., et al., *J. Inorg. Biochem.*, 2004, vol. 8, p. 313.
8. Zhang, H., Liu, C.S., Bu, X.H., and Yang, M., *J. Inorg. Biochem.*, 2005, vol. 99, p. 1119.
9. Travnicek, Z., Krystof, V., and Sipl, M., *J. Inorg. Biochem.*, 2006, vol. 100, p. 214.
10. Sheng, X., Guo, X., Lu, X.M., et al., *Bioconjugate Chem.*, 2008, vol. 19, p. 490.
11. Tan, J., Wang, B., and Zhu, L., *Bioorg. Med. Chem.*, 2009, vol. 17, p. 614.
12. Jiang, Q., Zhu, J., Zhang, Y., et al., *BioMetals*, 2009, vol. 22, p. 297.
13. Nakayama, A., Hiromura, M., Adachi, Y., and Sakurai, H., *J. Biol. Inorg. Chem.*, 2008, vol. 13, p. 675.
14. Sakurai, H., Yoshikawa, Y., and Yasui, H., *Chem. Soc. Rev.*, 2008, vol. 37, p. 2383.
15. Emami, S., HosseiniMehr, J., Taghdisi, S.M., and Akhlaghpour, S., *Bioorg. Med. Chem. Lett.*, 2007, vol. 17, p. 45.
16. Burlov A.S., Vlasenko V.G., Garnovskii D.A., Uraev A.I., Maltsev A.I., Lypenko D.A., Vannikov A.V. Electroluminescent Light-Emitting Diodes Based on Metal Coordination Compounds. SFedU, Rostov-on-Don, 2015 [in Russian] p. 232.
17. Sano, T., Nishio, Y., Hamada, Y., et al., *J. Mater. Chem.*, 2000, vol. 10, p. 157.
18. Kim, S.M., Kim, J.S., Shin, D.M., et al., *Bull. Kor. Chem. Soc.*, 2001, vol. 22, no. 7, p. 743.
19. Zhu, D., Su, Z., Mu, Z., et al., *J. Coord. Chem.*, 2006, vol. 59, no. 4, p. 409.
20. Amendola, V., Fernandez, Y.D., Mangano, C., et al., *Dalton Trans.*, 2003, p. 4340.
21. Yu, G., Liu, Y., Song, Y., et al., *Synth. Met.*, 2001, vol. 117, p. 211.
22. Chantarasiri, N., Ruangpornvisuti, V., Muangsin, N., et al., *J. Mol. Struct.*, 2004, vol. 701, p. 93.
23. Yu, T., Su, W., Li, W., et al., *Inorg. Chim. Acta*, 2006, vol. 359, p. 2246.
24. Yu, T., Zhang, K., Zhao, Y., et al., *Inorg. Chim. Acta*, 2008, vol. 361, p. 233.
25. Wang, P., Hong, Z., Xie, Z., et al., *Chem. Commun.*, 2003, p. 1664.
26. Bormejo, M.R., Vazques, M., Sanmartín, J., et al., *New J. Chem.*, 2002, vol. 26, p. 1365.
27. Metelitsa, A.V., Burlov, A.S., Bezuglyi, S.O., et al., RF Patent No. 2295527, *Byull. Izobret.*, 2007, no. 8.
28. Metelitsa, A.V., Burlov, A.S., Bezuglyi, S.O., et al., *Russ. J. Coord. Chem.*, 2006, vol. 32, no. 12, p. 858.
29. Burlov, A.S., Vlasenko, V.G., Garnovskii, D.A., et al., *Russ. J. Inorg. Chem.*, 2014, vol. 59, no. 7, p. 721.
30. Chernova, N.I., Ryabokobylko, Yu.S., Brudz', V.G., and Bolotin, B.M., *Zh. Org. Khim.*, 1971, vol. 7, no. 8, p. 1680.
31. Chernyshov, A.A., Veligzhanin, A.A., and Zubavichus, Y.V., *Nucl. Instrum. Methods Phys. Res. A*, 2009, vol. 603, p. 95.
32. Newville, M., *J. Synchrotron Rad.*, 2001, no. 8, p. 96.
33. Zabinski, S.I., Rehr, J.J., Ankudinov, A., and Alber, R.C., *Phys. Rev.*, 1995, vol. 52, p. 2995.
34. Frisch, M.J., Trucks, G.W., Schlegel, H.B., et al., *Gaussian 03. Revision A.1*, Pittsburgh: Gaussian, Inc., 2003.
35. Lee, C., Yang, W., and Parr, R.G., *Phys. Rev.*, 1988, vol. 37, p. 785.
36. Becke, A.D., *J. Chem. Phys.*, 1993, vol. 98, p. 5648.
37. Ditchfield, R., Hehre, W.J., and Pople, J.A., *J. Chem. Phys.*, 1971, vol. 54, no. 2, p. 724.
38. Dunning, T.H., Jr. and Hay, P.J., in *Modern Theoretical Chemistry*, Schaefer, H.F., III, Ed., New York: Plenum, 1977, vol. 3, p. 1.
39. *CrysAlisPro*, Agilent Technologies, Version 1.171.36.32.
40. Sheldrick, G.M., *Program for the Refinement of Crystal Structures*, Göttingen: Univ of Göttingen, 1997.
41. Bermejo, M.R., Sanmartín, J., Garcia-Deibe, A.M., et al., *Inorg. Chim. Acta*, 2003, vol. 3, p. 53.
42. Sousa-Pedrares, A., Viqueira, J.A., Antanelo, J., et al., *Eur. J. Inorg. Chem.*, 2011, p. 2273.
43. Popov, L.D., Levchenkov, S.I., Shcherbakov, I.N., et al., *Russ. J. Coord. Chem.*, 2013, vol. 39, no. 4, p. 342.

Translated by E. Yablonskaya